

Study of Band Structure: a DFT based Calculation for CeAs

By

Reg. No. 2016132056

B. Sc. 8th Semester Examination–2020 (held in 2021)

Session: 2016-2017

**A project work submitted to the Department of Physics as a
partial fulfillment of the requirement for the degree of
Bachelor of Science (B. Sc.)**



Department of Physics

School of Physical Sciences

Shahjalal University of Science and Technology

Sylhet, Bangladesh

March, 2021

Abstract

In the present work we have determined band structure of a solid material using a simple model potential. The model is called Kronig-Penny model where the calculated band energy is a function of wave number. We have made various calculation under this model by solving central polynomial equations using python 3.0 and also plot the curve y vs αa for $P = 1.5 \pi$ and other necessary graphs with the software Igor Pro Version 8.0. Density Functional Theory (DFT) was also discussed and applied to calculate and analyze the band structure of crystalline solid CeAs using DFT based CASTEP computer program with GGA and PBE exchange correlation functional.

Table of Contents

Chapter 1	1
Introduction	1
Chapter 2	3
Origin of Energy Bands	3
2.1 Energy Levels	3
2.2 Energy Bands	5
Chapter 3	10
Band Energy Calculation: The Kronig-Penney Model	10
3.1 The crystal potential	10
3.2 The Bloch Theorem	11
3.3 The Kronig-Penney (KP) model	12
3.4 The Central Equation	15
3.5 Energy versus Wave number curves	18
3.6 Different Zone Schemes	19
Chapter 4	20
Other Models for Deciding Band Energy	20
4.1 The Nearly-free Electron Model	20
4.2 The Tight-binding Model	23
4.3 The Wigner-Seitz Method	24
Chapter 5	26
Density Functional Theory (DFT)	26
5.1 Basic Idea of DFT	26
5.2 Parameters Used	27
Chapter 6	28
Calculation of Band Energy	28
6.1 Calculation for K-P Model	28
6.1.1 Generation of y versus αa Data	28
6.1.2 Plotting y versus αa Data	29
6.1.3 Band Energy Calculation	29
6.2 DFT-based Calculation for Band Energy of CeAs	32
Chapter 7	34
Results and Discussion	34

7.1 Band Energy of KP Model	34
7.1.1 Band Energy versus Wave Number Curves	34
7.1.2 Variation of Band Gap with P	35
7.2 Band Energy of CeAs based on DFT	36
Chapter 8	34
Conclusion	39
References	40

Chapter 1

Introduction

Chapter 1

Introduction

In solid state physics, the electronic band structure of a solid describes the range of energy levels that electrons may have within it, as well as the ranges of energy that may not have. Band theory derives these bands and band gaps by examining the allowed quantum mechanical wave functions for an electron in a large, periodic lattice of atoms or molecules. Band theory has been successfully used to explain many physical properties of solids, such as electrical resistivity and optical absorption etc.

If a large number of identical atoms come together to form a solid, such as crystal lattice, the atoms' atomic orbitals overlap. Then each atomic orbital splits into N discrete molecular orbitals, each with different energy. The adjacent levels are so close together that they can be considered as a continuum, an energy band.

The aim of this project is to determine the band structure of a solid material using a simple model potential. There are many models for calculating band structure of a solid material, such as Kronig-Penny Model, Nearly Free Electron model, Tight Binding Model, and so on.

We have calculated band energy as a function of wave number using Kronig-Penny Model [1-3]. But we have described the other models in this report, although in brief. The Kronig-Penny model is normally a one dimensional rectangular well model useful for illustration of band formation. While simple, it predicts many important phenomena, but is not quantitative. We have made various calculations under this model using Igor Pro Version 8.0 software [4].

In the last few decades, scientists are adopting density functional theory (DFT) for calculating the band structure and many other properties of materials. Thomas-Fermi model [5] gave the original idea/clue of DFT. This theory has been developed by P. Hohenberg and W. Kohn [6] and W. Kohn and L. J. Sham [7]. DFT replaces the complicated N -electron wavefunction and corresponding Schrödinger in much simpler form. The wavefunction is replaced by electron density. Our calculations for band structures were carried out using the DFT-based CASTEP computer program together with the generalized gradient approximation (GGA) and the PBE exchange-correlation functional [8-11].

The planning of the treatise has been done as follows. The topics related to this work, such as, energy levels, energy bands are presented in Chapter 2. Discussion about crystal potential, Bloch theorem, The Kronig-Penny Model along with its central equation, energy vs wavenumber curves, different zone schemes are discussed in Chapter 3. The other models of band energy such as nearly free electron model, tight binding model, Wigner-Seitz model are briefly discussed in Chapter 4. The calculation of band energy is in Chapter 5 where we will discuss the procedure used in this calculation using a software named Igor Pro 8 and Python 3. Chapter 6 is presented with a discussion about the basic idea of Density Functional Theory, parameter used in it, and the band structure of CeAs. Result and Discussion is included in Chapter 7. And a brief conclusion is drawn in Chapter 8

Chapter 2

Origin of Energy Bands

Chapter 2

Origin of Energy Bands

In a single isolated atom, the electrons in each orbit have definite energy associated with it. But in case of solids all the atoms are close to each other, so the energy levels of outermost orbit electrons are affected tremendously by the neighboring atoms.

2.1 Energy Levels

An atom has three major parts which are protons, electrons and neutrons. Where the charge of the electrons is negative and the charge of the protons are positive. Though both the proton and electron have same amount of charge, proton has greater mass than electron. And a neutron is neutral in charge and has a mass nearly equal to proton. The entire mass of the atom is practically the total mass of proton and neutron and it is called atomic nucleus. In an atom, the electrons revolve round the nucleus in definite orbits (circular or elliptical).

According to Bohr atomic model, the allowed circular orbit of any revolving electron around the nucleus is given by the condition

$$\text{Angular momentum of the electron} = n\hbar \quad [n = 1, 2, 3, \dots]$$

The energies of electrons corresponding to $n = 1, 2, 3, \dots$ can also be represented by horizontal lines in a diagram, called the *energy level diagram* of the atom (Figure 2.1).

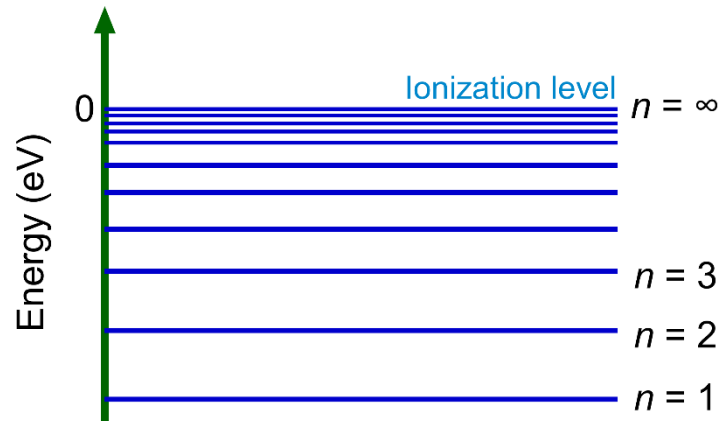


Figure 2.1: Energy levels of electrons in an atom.

When an electron jumps from a higher energy level E_h to a lower energy level E_l an electromagnetic radiation of frequency ν is emitted, where

$$\nu = \frac{E_h - E_l}{h} \quad (2.1)$$

where h is Planck's constant ($h = 6.62 \times 10^{-34}$ J.s).

On the contrary, on absorbing a photon of energy $h\nu$, an electron initially at the energy state E_l can move to the energy state E_h .

An electron normally occupies the lowest energy state, called the *ground level*, the other higher lying energy levels are called the *excited levels* of the atom. By absorbing energies, an electron jumps into excited states which are farther away from the nucleus. The energy required for this to occur is known as the *ionization potential*. The ionization level represents the zero level of energy.

Quantum mechanical treatments of electrons in an atom have introduced four *quantum numbers*, designated by n , l , m_l and m_s . The quantum numbers can take the following values:

$$n = 1, 2, 3, \dots$$

$$l = 0, 1, 2, 3, \dots, (n - 1)$$

$$m_l = 0, \pm 1, \pm 2, \dots, \pm l$$

$$\text{and } m_s = \pm \frac{1}{2}$$

Here,

(i) n , the *principal quantum number*, primarily determines the energy of the orbital electrons.

(ii) l , *orbital angular momentum quantum number*, measures the angular momentum of the electron,

(iii) m_l , *magnetic quantum number*, gives the splitting of the energies for a given n and l in a magnetic field.

(iv) m_s , known as the *spin quantum number*, shows that the spin of the electron about its own axis is quantized.

The specific value of the principal quantum number n determines an electronic shell. The letters K, L, M, N, ... denote the shells for $n = 1, 2, 3, 4$, respectively. The subshells are denoted by s, p, d, f .

2.2 Energy Bands

When two single or isolated atoms are brought close to each other than the outermost orbit electrons of two atoms interact with each other. i.e. the electrons in the outermost orbit of one atom experience an attractive force from the nearest or neighboring atomic nucleus. Due to this the energies of the electrons will not be in same level, the energy levels of electrons are changed to a value which is higher or lower than that of the original energy

Energy bands occur in solids where the discrete energy levels of the individual atoms merge into bands which contain a large number of closely spaced energy levels. Energy bands consisting of a large number of closely spaced energy levels exist in crystalline materials.

The Pauli exclusion principle does not allow the electron energy levels to be the same so that one obtains a set of closely spaced energy levels, forming an energy band. The energy band model is crucial to any detailed treatment of semiconductor devices. It provides the framework needed to understand the concept of an energy band gap.

Let consider an isolated atom of atomic number Z , the atomic nucleus has a positive charge Ze . The electrostatic potential (in SI units) at a distance r from the nucleus due to the nuclear charge Ze is given by

$$V(r) = \frac{Ze}{4\pi\epsilon_0 r} \quad (2.2)$$

where ϵ_0 is the permittivity of free space.

The potential energy $U(r)$ of an electron at a distance r from the nucleus is written as

$$U(r) = -eV(r) = -\frac{Ze^2}{4\pi\epsilon_0 r} \quad (2.3)$$

Fig. 2.2 shows the potential energy $U(r)$ of an electron with distance r from the nucleus of an isolated atom. Whereas, potential energy felt by an electron, $U(r)$, as a function distance r for a row of atoms in a crystal is shown in Fig 2.3.

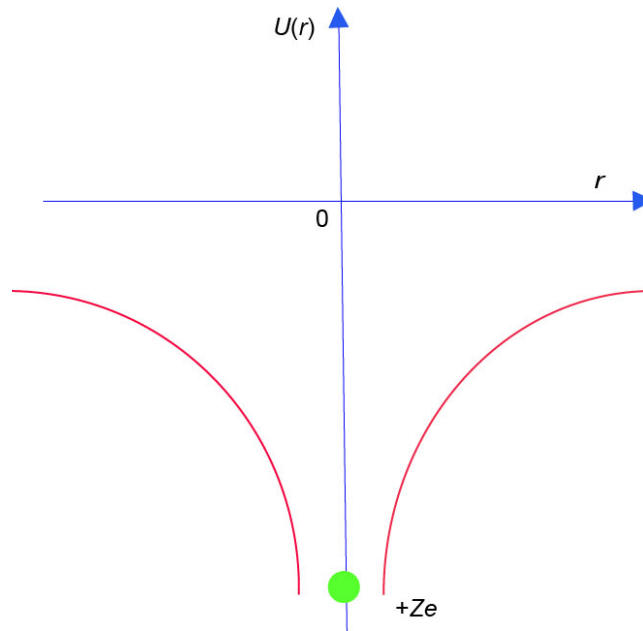


Figure 2.2: Potential energy $U(r)$ of an electron with distance r from the nucleus of an isolated atom.

It is seen from Eq. (2.3) that $U(r)$ is zero at an infinite distance from the nucleus. The total energy (kinetic plus potential) of an electron in an atom has discrete values, called discrete energy levels. In a crystal, the neighboring atoms experience electric force on each other, and hence it is considered as a single electronic system obeying Pauli's exclusion principle.

In order to satisfy the Pauli's exclusion principle, each energy level of the isolated atom splits into as many energy levels as there are atoms in the crystal with very small split-off energy. This large number of discrete and closely spaced energy levels form an *energy band*. Energy bands are represented schematically by shaded regions in Fig. 2.4.

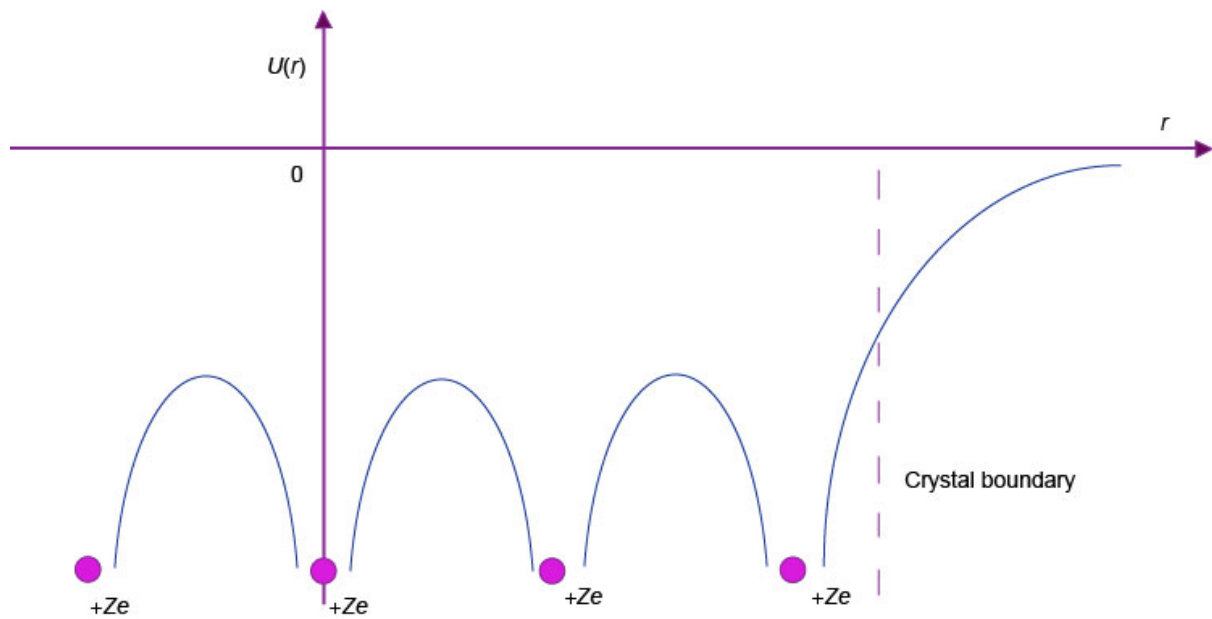


Figure 2.3: Potential energy felt by an electron, $U(r)$, as a function distance r for a row of atoms in a crystal.

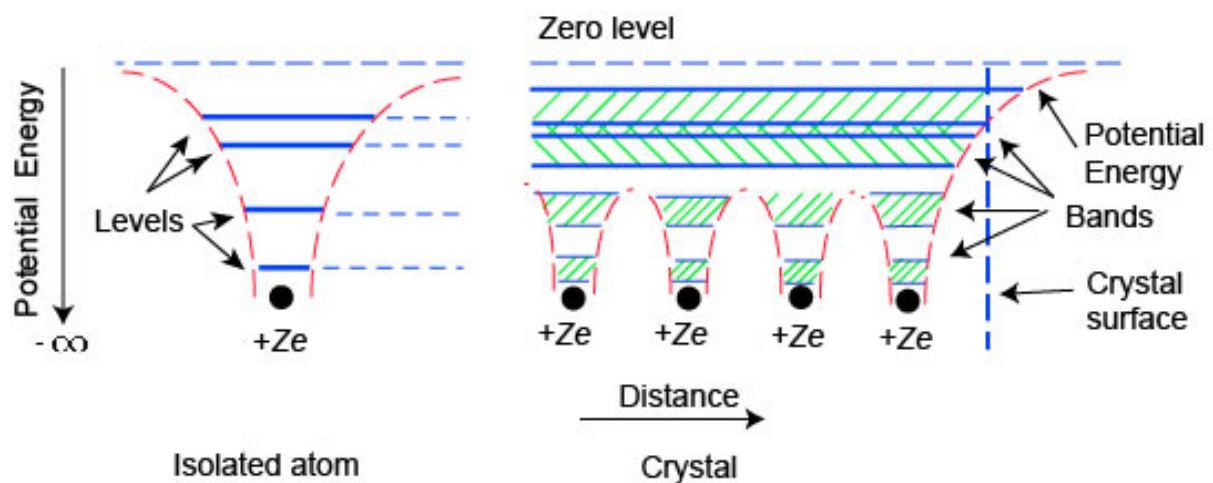


Figure 2.4: Conversion of energy levels of isolated atoms into energy bands if they are in a crystal.

The higher energy levels are greatly affected by the interatomic interactions and produce wide bands. The width of an energy band thus depends on the type of the crystal, and is larger for a crystal with a small interatomic spacing and also independent of the number of atoms in the

crystal, but the number of energy levels in a band is equal to the number of atoms in the solid.

As the number of atoms in the crystal increases, the separation between the energy levels in a band decrease. As the crystal contains a large number of atoms ($\approx 10^{29} \text{ m}^{-3}$), the spacing between the discrete levels in a band is so small that the band can be treated as continuous.

The lower energy bands are normally completely filled by the electrons since the electrons always tend to occupy the lowest available energy states. The higher energy bands may be completely empty or may be partly filled by the electrons. As the allowed energy levels of a single atom expand into energy bands in a crystal, the electrons in a crystal cannot have energies in the region between two successive bands. In other words, the energy bands are separated by gaps of *forbidden energy*. This fact will be clearly realized from the findings of Kronig-Penney model (Chapter 3).

The rise of the potential energy near the surface of the crystal, as shown in Fig. 2.4, serves as a *barrier* preventing the electrons from escaping from the crystal. If sufficient energy is imparted to the electrons by external means, they can overcome the surface potential energy barrier, and come out of the crystal surface.

Chapter 3

Band Energy Calculation: The Kronig-Penney Model

Chapter 3

Band Energy Calculation: The Kronig-Penney Model

3.1 The crystal potential

From a quantum mechanical point of view, the motion of an electron in a crystal is considered to be based on the Schrödinger equation

$$\left[-\frac{\hbar^2}{2m} \nabla^2 + V(\mathbf{r}) \right] \psi(\mathbf{r}) = E\psi(\mathbf{r}) \quad (3.1)$$

where $V(\mathbf{r})$, $\psi(\mathbf{r})$ and E are the crystal potential felt by the electron, the state function and energy of the electron, respectively

The crystal may be surveyed as a periodic arrangement of ion cores which are positively-charged containing the nuclei and non-valence electrons that may be assumed stationary in the lattice points.

The potential of a valence electron in a single isolated atom is shown in Fig. 3.1

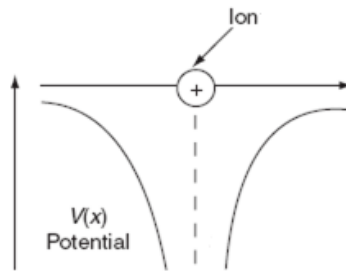


Fig. 3.1: The potential $V(\mathbf{r})$ of a valence electron around in an isolated atom.

The periodic potential $V(\mathbf{r})$ has the same translational symmetry as the lattice, i.e.,

$$V(\mathbf{r} + \mathbf{R}) = V(\mathbf{r}), \quad (3.2)$$

where \mathbf{R} is the lattice vector.

The potential can be showed in the following diagram.

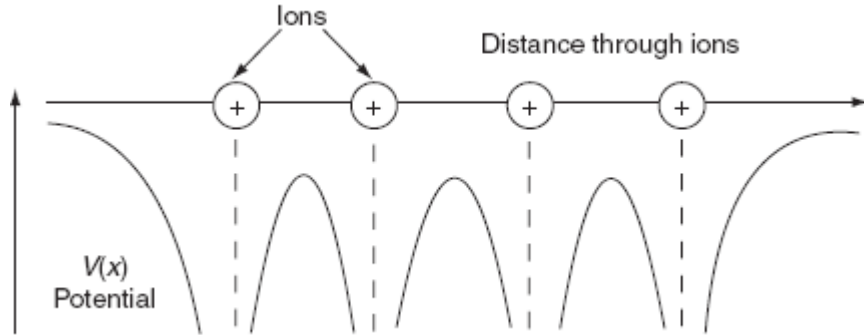


Fig. 3.2: The potential for one-dimensional periodic array of atoms.

3.2 The Bloch Theorem

According to Bloch theorem the wavefunction associated with the moving electron in a periodic potential can be written as [3]

$$\psi_k(\mathbf{r}) = u_k(\mathbf{r})e^{i\mathbf{k}\cdot\mathbf{r}}, \quad (3.3)$$

where the function $u_k(\mathbf{r})$ has the same translational symmetry as the crystal lattice, that is,

$$u_k(\mathbf{r}) = u_k(\mathbf{r} + \mathbf{R}) \quad (3.4)$$

$u_k(\mathbf{r})$ is a periodic function which possesses the periodicity of the lattice in the r -direction. Therefore, $u_k(\mathbf{r})$ changes periodically with increasing r (modulated amplitude). Of course, $u_k(\mathbf{r})$ is different for various directions in the crystal lattice.

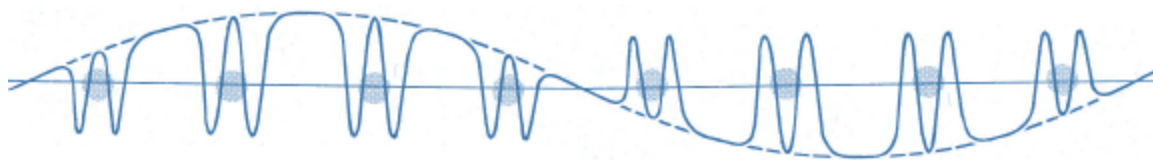


Figure 3.3: The Bloch function. The smooth dashed curve represents the wave $e^{i\mathbf{k}\cdot\mathbf{r}}$

The result of equation (3.3) is called the Bloch theorem. According to Bloch Theorem, the product of a plane wave $e^{ik \cdot r}$ and the periodic function $u_k(\mathbf{r})$ is considered as the eigenfunctions of the wave equation.

3.3 The Kronig-Penney (KP) model

The Kronig-Penney (KP) model is known as a single-electron problem. The electron moves in a one-dimensional crystal. The following periodical function approximates the periodic potential experienced by the electrons in the crystal.

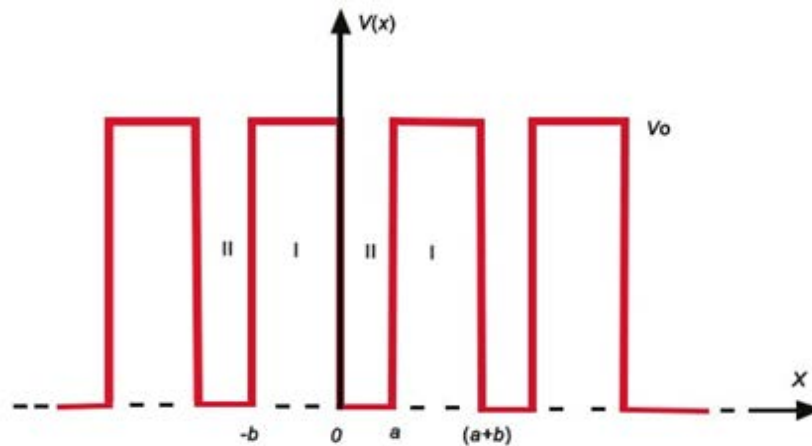


Figure 3.4: The Kronig-penny model potential.

Kronig and Penny approximated the potential energy of electron inside the crystal to the shape of rectangular steps while moving in one dimensional crystal lattice.

The regions denoted II correspond to the positively charged ions of the crystal lattice, where potential energy $V=0$.

The regions denoted I represent the empty spaces between the ions where $V=V_0$.

It is the choice of this oversimplified potential that makes an analytical solution possible. The lattice parameter is $(a+b)$.

The single-electron problem is described by the Schrödinger equation in the regions $0 < x < a$ & $-b < x < 0$.

$$-\frac{\hbar^2}{2m} \frac{d^2\psi}{dx^2} + V(x)\psi = E\psi \quad (3.5)$$

Equation (3.5) can be given separately for regions I and II:

$$\frac{d^2\psi}{dx^2} + \frac{2m}{\hbar^2} E\psi = 0 \text{ (for region II)} \quad (3.6)$$

and

$$\frac{d^2\psi}{dx^2} + \frac{2m}{\hbar^2} (E - V_0)\psi = 0 \text{ (for region I)} \quad (3.7)$$

The general solutions are

$$\frac{d^2\psi}{dx^2} + \alpha^2\psi = 0 \text{ (for } 0 < x < a), \quad (3.8)$$

$$\text{where } \alpha^2 = \frac{2mE}{\hbar^2}$$

$$\frac{d^2\psi}{dx^2} - \beta^2\psi = 0 \text{ (for } -b < x < a), \quad (3.9)$$

$$\text{where } \beta^2 = \frac{2m}{\hbar^2} (V_0 - E)$$

Since the potential is periodic, so the solution of eq. (3.8) and (3.9) must be of the form of Bloch functions i.e.

$$\psi = u_k(x)e^{ikx} \quad (3.10)$$

Where $u_k(x)$ is the periodic function of x with period $(a + b)$.

$$\text{Now, } \frac{d\psi}{dx} = ike^{ikx}u_k(x) + e^{ikx}\frac{du}{dx}$$

$$\frac{d^2\psi}{dx^2} = -k^2e^{ikx}u_k(x) + ike^{ikx}\frac{du}{dx} + ike^{ikx}\frac{du}{dx} + e^{ikx}\frac{d^2u}{dx^2}$$

$$= -k^2 e^{ikx} u_k(x) + 2ike^{ikx} \frac{du}{dx} + e^{ikx} \frac{d^2 u}{dx^2}$$

Substituting the value of $\frac{d^2 \psi}{dx^2}$ in eq. (3.8) and (3.9) we get

$$\frac{d^2 u_1}{dx^2} + 2ik \frac{du_1}{dx} + (\alpha^2 - k^2) u_1 = 0 \text{ (for } 0 < x < a \text{)} \quad (3.11)$$

$$\frac{d^2 u_2}{dx^2} + 2ik \frac{du_2}{dx} - (\beta^2 + k^2) u_2 = 0 \text{ (for } -b < x < 0 \text{)}, \quad (3.12)$$

where u_1 represents the value of $u_k(x)$ in the region $0 < x < a$ & u_2 in the region $-b < x < 0$.

To solve the differential equation in (3.11) we assume $u_1 = e^{mx}$. Thus

$$\frac{du_1}{dx} = me^{mx} \text{ \& } \frac{d^2 u_1}{dx^2} = m^2 e^{mx}.$$

Substituting the values of $\frac{du_1}{dx}$ & $\frac{d^2 u_1}{dx^2}$ in equation (3.11) we get

$$m^2 e^{mx} + 2ikme^{mx} + (\alpha^2 - k^2) e^{mx} = 0$$

$$\text{Or, } m^2 + 2ikm + (\alpha^2 - k^2) = 0$$

This equation can be solved for m as follows

$$\begin{aligned} m &= \frac{-2ik \pm \sqrt{(2ik)^2 - 4.1.(\alpha^2 - k^2)}}{2.1} \\ &= \frac{-2ik \pm \sqrt{-4k^2 - 4\alpha^2 + 4k^2}}{2} \\ &= \frac{-2ik \pm 2i\alpha}{2} = -ik \pm i\alpha \end{aligned}$$

So the two roots of m are, $m_1 = i(\alpha - k)$ & $m_2 = -i(\alpha + k)$

Hence the general solution is

$$u_1 = Ae^{m_1 x} + Be^{m_2 x}$$

$$\text{Or, } u_1 = Ae^{i(\alpha - k)x} + Be^{-i(\alpha + k)x} \quad (3.13)$$

A similar treatment for u_2 gives

$$u_2 = C e^{(\beta - ik)x} + D e^{-(\beta + ik)x}, \quad (3.14)$$

where A, B, C, D are constants

3.4 The Central Equation

In equation (3.13) & (3.14), A, B, C and D are arbitrary constants which can be determined by the following boundary conditions

$$(i) (u_1)_{x=0} = (u_2)_{x=0}$$

$$\text{Or, } A + B = C + D \quad (3.15)$$

$$(ii) (u_1')_{x=0} = (u_2')_{x=0}$$

$$\text{Or, } i(\alpha - k)A - i(\alpha + k)B =$$

$$(\beta - ik)C - (\beta + ik)D \quad (3.16)$$

$$(iii) (u_1)_{x=a} = (u_2)_{x=-b}$$

$$[\because u_2(a) = u_2(a - (a + b)) = u_2(-b)]$$

$$\text{Or, } A e^{i(\alpha - k)a} + B e^{-i(\alpha + k)a} =$$

$$C e^{-(\beta - ik)b} + D e^{(\beta + ik)b} \quad (3.17)$$

$$(iv) (u_1')_{x=a} = (u_2')_{x=-b}$$

$$\text{Or, } i(\alpha - k)A e^{i(\alpha - k)a} - i(\alpha + k)B e^{-i(\alpha + k)a} =$$

$$(\beta - ik)C e^{-(\beta - ik)b} - (\beta + ik)D e^{(\beta + ik)b} \quad (3.18)$$

The coefficients A, B, C, D can be determined by solving equations (3.15) through (3.18), and using those, the wave functions $\psi_1 = u_1 e^{ikx}$ & $\psi_2 = u_2 e^{ikx}$ may be evaluated utilizing equations (3.13) & (3.14).

Equations (3.15) to (3.18) can be solved for non-zero values of A , B , C and D only if the determinant of the coefficient of A , B , C and D becomes zero.

$$\begin{vmatrix} 1 & 1 & -1 & -1 \\ i(\alpha - k) & -i(\alpha + k) & -(\beta - ik) & (\beta + ik) \\ e^{i(\alpha - k)a} & e^{-i(\alpha + k)a} & -e^{-(\beta - ik)b} & -e^{(\beta + ik)b} \\ i(\alpha - k)e^{i(\alpha - k)a} & -i(\alpha + k)e^{-i(\alpha + k)a} & -(\beta - ik)e^{-(\beta - ik)b} & (\beta + ik)e^{(\beta + ik)b} \end{vmatrix} = 0$$

On solving, we get

$$\frac{\beta^2 - \alpha^2}{2\alpha\beta} \sinh \beta b \sin \alpha a + \cosh \beta b \cos \alpha a = \cos k(a + b) \quad (3.19)$$

In order to make the situation simpler, Kronig and Penney considered the height of the potential barrier is very large. i.e. $V_0 \rightarrow \infty$ and simultaneously the width of the barrier $b \rightarrow 0$ in such a way that the product $V_0 b$ remain finite.

In the limit, $V_0 \rightarrow \infty$, we can write

$$\beta^2 = \frac{2m}{\hbar^2} (V_0 - E) \approx \frac{2mV_0}{\hbar^2}$$

We assumed earlier, $\alpha^2 = \frac{2mE}{\hbar^2}$

Comparing these two we can safely assign the relation: $\beta \gg \alpha$ as $V_0 \gg E$.

In the limit, $b \rightarrow 0$, we have $\beta b \ll 1$

$$\therefore \sinh \beta b = \frac{e^{\beta b} - e^{-\beta b}}{2} = \frac{1 + \beta b - (1 - \beta b)}{2} = \beta b$$

$$\text{and } \cosh \beta b = \frac{e^{\beta b} + e^{-\beta b}}{2} = \frac{1 + \beta b + (1 - \beta b)}{2} = 1$$

Under the circumstances equation (3.19) becomes,

$$\frac{\beta^2 b}{2\alpha} \sin \alpha a + \cos \alpha a = \cos ka$$

$$\text{Or, } \frac{P}{\alpha a} \sin \alpha a + \cos \alpha a = \cos ka, \quad (3.20)$$

$$\text{where } P = \frac{\beta^2 ab}{2} = \frac{2mV_0 ab}{2\hbar^2} = \frac{mV_0 ab}{\hbar^2}$$

Thus, P is a measure of the quantity $V_0 b$ (the area of the potential barrier).

If a graph of the function $\frac{P}{\alpha a} \sin \alpha a + \cos \alpha a$ is plotted against αa for $P = \frac{3\pi}{2}$, a curve as shown in Figure 3.5 is obtained.

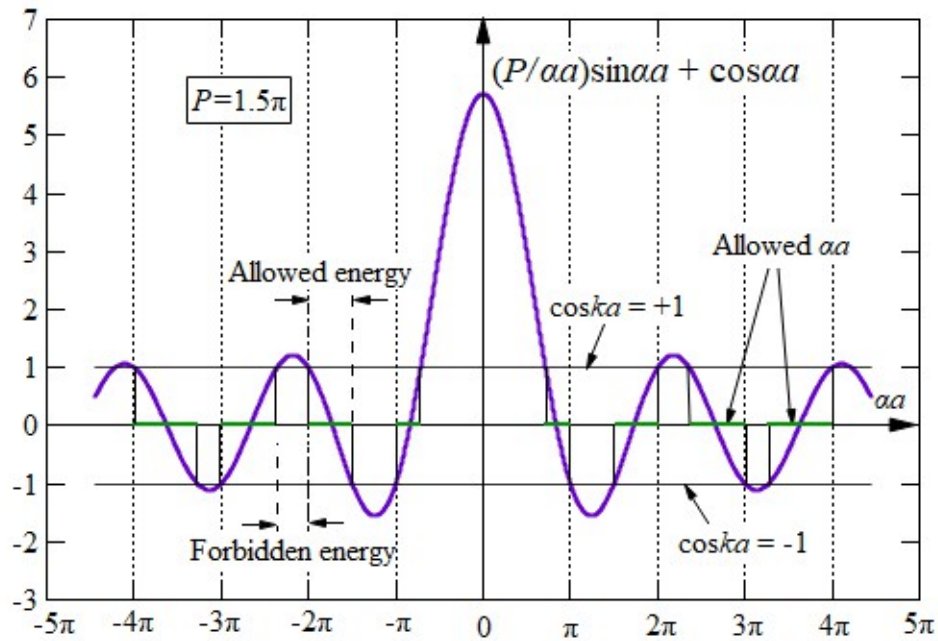


Figure 3.5: Plot of the function $\frac{P}{\alpha a} \sin \alpha a + \cos \alpha a$ as a function of αa for $P = \frac{3\pi}{2}$.

3.5 Energy versus Wave number curves

Equation (3.20) can only be solved numerically. Solutions are only obtained if the value of $\cos ka$ is between -1 and 1. Since $\alpha = \sqrt{\frac{2mE}{\hbar^2}}$, we can see that αa is a measure of energy. The allowed values of αa , corresponding to parts of the curve of $\frac{P}{\alpha a} \sin \alpha a + \cos \alpha a$ versus αa lying between $\cos ka = \pm 1$, are indicated in Figure 3.5 by bold lines. The energy spectrum of the electron consists of alternate regions of allowed energy bands & forbidden energy bands.

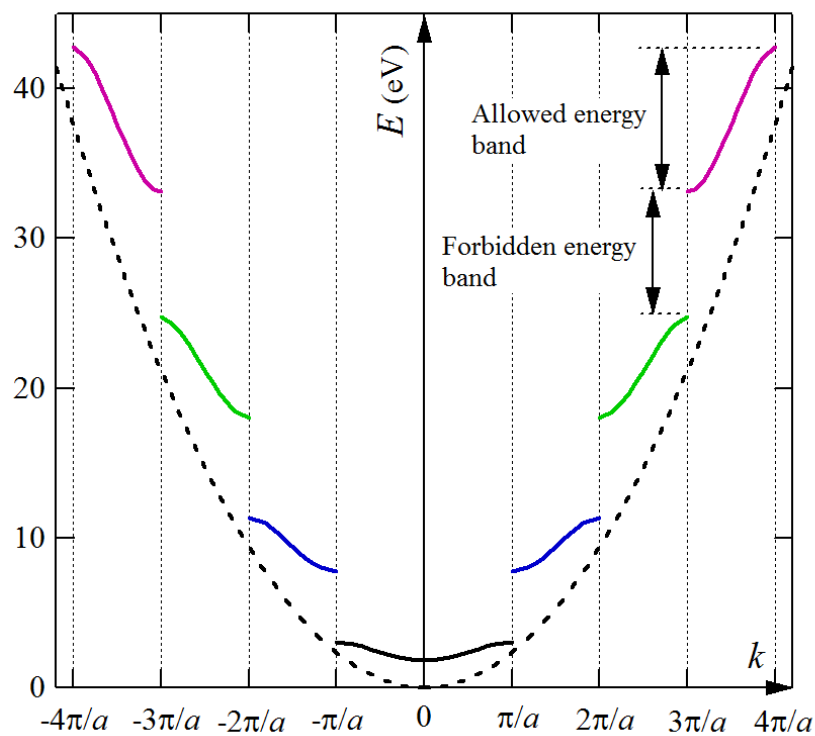


Figure 3.6: Energy E versus wavenumber k curves for the Kronig-Penney potential with $P = 3\pi/2$ (solid curves) in the extended zone scheme. Dashed curve is E versus k curve (a parabola) for free electrons ($P = 0$).

The boundaries of the allowed ranges of ka corresponds to the values of

$$\cos ka = \pm 1$$

$$\text{Or, } ka = \pm n\pi$$

$$\text{Or, } k = \pm \frac{n\pi}{a}; (n = 0, 1, 2, 3, \dots, \text{etc.}) .$$

The energy, E , is plotted as function of wavenumber k in Figure 3.6.

3.6 Different Zone Schemes

In the *Extended zone scheme*. Different bands are mapped in different zones in the wave vector space (Figure 3.6).

In the *Reduced zone scheme*, all bands are mapped in the first Brillouin zone. In this zone, we may find different energies at the same value of wave vector. Each different energy characterizes a different band.

If every band is mapped in every zone, then it is known as *periodic zone scheme*.

Chapter 4

Other Models for Deciding Band Energy

Chapter 4

Other Models for Deciding Band Energy

4.1 The Nearly-free Electron Model

In this section we will discuss about nearly free electron model (NFE). According to this model, it is assumed that the electron behaves as free particle because of the weak crystal potential. And then, the perturbation method is applied to deal with the effects of potential [11].

The starting point of NFE model is the solution of the Schrodinger equation in the case of zero potential.

$$\frac{-\hbar^2}{2m} \frac{d^2\psi}{dx^2} + V(x)\psi = E\psi$$

In nearly-free electron approximation $V(x)$ is small compared with the kinetic energy.

When we treat the potential; $V(x)$ as a perturbation, the perturbed energy $E_1^{(0)}(k)$ up to the second order of the potential given by

$$E_1(k) = E_1^{(0)}(k) + \langle \psi_{1,k}^{(0)} | V | \psi_{1,k}^{(0)} \rangle + \sum'_{k',n} \frac{|\langle n,k' | V | 1,k \rangle|^2}{E_1^{(0)}(k) - E_1^{(0)}(k')} \quad (4.1)$$

Here, subscript 1 refers to the first band, which is one of interest, and the subscript 0 refers to empty lattice model equations

$$\psi_k^{(0)} = \frac{1}{L^{1/2}} e^{ikx} \quad (4.2)$$

$$E_1^{(0)}(k) = \frac{\hbar^2 k^2}{2m_0} \quad (4.3)$$

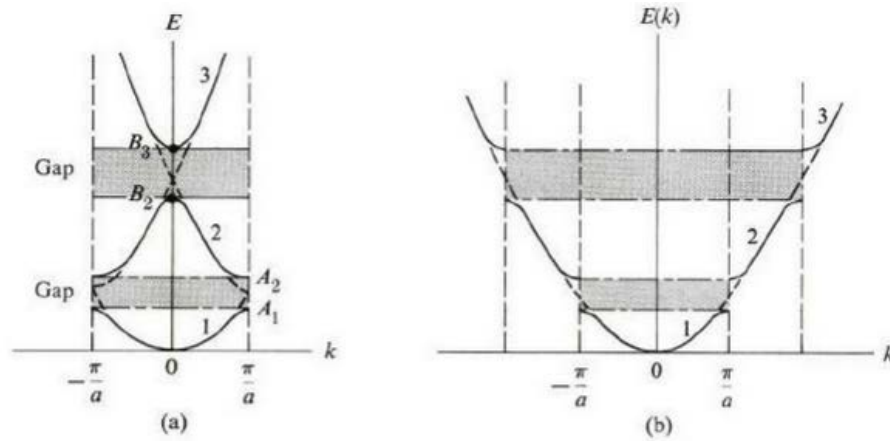


Figure 4.1: (a) Dispersion curves in the nearly free electron model in the reduced zone (b) the same dispersion curves in the extended – zone scheme

The second term of the right side of eq (4.1) which is a first order correction, is the average value of the potential. The third term, giving the second order correction, involves summing over all states nuke.

The first order correction can be written as

$$\langle \psi_{1,k}^{(0)} | V | \psi_{1,k}^{(0)} \rangle = \frac{1}{L} \int e^{-ikx} V(x) e^{ikx} dx = \frac{1}{L} \int V(x) dx \quad (4.4)$$

This is defined as the average value of potential over entire lattice, independent of k and merely a constant.as the terms do not lead to anything it will be set to zero by shifting the zero-energy level.

Considering the second-order correction, the quantity $\langle n, k' | V | 1, k \rangle$ can be vanished except when $k' = k$, where k and k' are restricted to the first zone. In the denominator an arbitrary potential $V(x)$ can always be expanded as Fourier Series

$$V(x) = \sum_k V_k e^{ikx} \quad (4.5)$$

The Fourier coefficient V_k given by

$$V_k = (1/L) \int_0^L V(x) e^{-ikx} dx \quad (4.6)$$

But if $V(x)$ is periodic then only $k=G$ contribute to the above summation that is $V_k=0$ for $K \neq G$.

Now the expansion $V(x) = \sum_G V_G e^{iGx}$

$$\text{We may write } E_1(k) \approx E^{(0)}_1(k) + \frac{|V_{-2\pi/a}|^2}{E^{(0)}_1(k) - E^{(0)}_2(k)} \quad (4.7)$$

Where $V_{-2\pi/a}$ is the Fourier component of the potential that is

$$V_{-2\pi/a} = (1/L) \int V(x) e^{+i(2\pi/a)x} dx \quad (4.8)$$

If the potential is weak, then $|V_{-2\pi/a}|^2$ is very small and the second term in equation (4.7) is negligible. In other words, $E_1(k) \approx E^{(0)}_1(k)$ and the effect of the lattice potential is negligible.

According to eq (4.7) In the point $k=\pi/a$ at the zone edge, the perturbation correction become large. So in this neighborhood we applied degenerate perturbation theory in which both bands 1 and 2 are treated equally. The resulting values are

$$E_{\pm}(k) = \left(\frac{1}{2}\right) \left\{ E^{(0)}_1(k) + E^{(0)}_2(k) \pm \left[(E^{(0)}_2(k) - E^{(0)}_1(k))^2 + 4 \left| V_{-\frac{2\pi}{a}} \right|^2 \right]^{\frac{1}{2}} \right\} \quad (4.9)$$

Plus sign denotes the upper band (band2) and minus sign denotes the lower band(band1). And the energy gap become

$$E_g = 2|V_{-2\pi/a}|$$

which is twice the Fourier component of the crystal potential.

Now, applying the degenerate formula (4.1) to the splitting of the bands 2,3 at the center of the zone, for small $k \ll \pi/a$

$$E_3(k) = E_B + \left| V_{-\frac{4\pi}{a}} \right| + \frac{\hbar^2}{2m_o} \alpha k^2 \quad (4.10)$$

And
$$E_2(k) = E_B - \left| V_{-\frac{4\pi}{a}} \right| - \frac{\hbar^2}{2m_o} \alpha k^2 \quad (4.11)$$

Here, the parameter α is given by

$$\alpha = 1 + \frac{4E_B}{E_g} \quad (4.12)$$

From these results, several reasons reveal

- i) From eq (4.9), an electron near the bottom of the third band $E \sim k^2$ which is similar to the dispersion relation of free electron, which says the electron there behaves like free electron. Effective mass given by $m^* = m_o/\alpha$
- ii) Eq (4.11) shows, for an electron near the top of the second band $E \sim -k^2$, which is like free electron but the effective mass is negative and the reason behind it is crystal potential and it's a frequent occurrence in solids.

4.2 The Tight-binding Model

In the tight-binding model we assume the opposite limit to that used for the nearly-free-electron approach, i.e., the potential is so large that the electrons spend most of their lives bound to ionic cores, only occasionally jump from one atom to another through quantum-mechanical tunneling.

The atomic wave functions $\phi_v(\mathbf{r})$ are defined by

$$H_{at}\phi_v(\mathbf{r}) = E_j\phi_v(\mathbf{r})$$

Where H_{at} is the Hamiltonian of a single atom.

The assumptions of this model are

1. Close to each lattice point, the crystal Hamiltonian H can be approximated by H_{at} .
2. The bound levels of H_{at} are well localized, i.e. the $\phi_v(\mathbf{r})$ are very small one lattice spacing away, implying that
3. $\phi_v(\mathbf{r})$ is quite a good approximation to a stationary state of the crystal, as will be $\phi_v(\mathbf{r} + \mathbf{R})$.

The Bloch function $\psi_k(\mathbf{r})$ of the electrons in the crystal according to this model can be written as the linear combinations of the atomic wave functions. Thus

$$\psi_k(\mathbf{r}) = \sum_{j=1}^N C_{kj} \phi_v(\mathbf{r} - \mathbf{R}_j), \quad (4.1)$$

where the sum is over all the lattice points.

This function is of the Bloch form if $C_{kj} = \frac{1}{\sqrt{N}} e^{i\mathbf{k} \cdot \mathbf{R}_j}$, where N is the total number of atoms in the crystal. Hence

$$\psi_k(\mathbf{r}) = \frac{1}{\sqrt{N}} \sum_{j=1}^N e^{i\mathbf{k} \cdot \mathbf{R}_j} \phi_v(\mathbf{r} - \mathbf{R}_j) \quad (4.2)$$

It is necessary to ascertain that this function is a Bloch function.

From equation (4.2) we can write,

$$\begin{aligned} \psi_k(\mathbf{r} + \mathbf{R}) &= \frac{1}{\sqrt{N}} \sum_{j=1}^N e^{i\mathbf{k} \cdot \mathbf{R}_j} \phi_v(\mathbf{r} + \mathbf{R} - \mathbf{R}_j) \\ &= e^{i\mathbf{k} \cdot \mathbf{R}} \frac{1}{\sqrt{N}} \sum_{j=1}^N e^{i\mathbf{k} \cdot (\mathbf{R}_j - \mathbf{R})} \phi_v(\mathbf{r} - (\mathbf{R}_j - \mathbf{R})) \\ &= e^{i\mathbf{k} \cdot \mathbf{R}} \frac{1}{\sqrt{N}} \sum_{j=1}^N e^{i\mathbf{k} \cdot \bar{\mathbf{R}}} \phi_v(\mathbf{r} - \bar{\mathbf{R}}) ; \text{ where } \bar{\mathbf{R}} = \mathbf{R}_j - \mathbf{R} \\ &= e^{i\mathbf{k} \cdot \mathbf{R}} \psi_k(\mathbf{r}) \end{aligned}$$

4.3 The Wigner-Seitz Method

The TB model is too crude to be useful in calculations of actual bands, which are to be compared with experimental results. Now we shall

consider some of the common methods employed in calculations of actual bands.

The cellular method was the earliest method employed in band calculations by Wigner and Seitz [12]. It was applied with success to the alkali metals, particularly to Na and K.

The Schrödinger equation whose solution we seek is

$$\left[\frac{\hbar^2}{2m} \nabla^2 + V(\mathbf{r}) \right] \psi_k(\mathbf{r}) = E(\mathbf{k}) \psi_k(\mathbf{r})$$

where $V(\mathbf{r})$ is the crystal potential and $\psi_k(\mathbf{r})$ is the Bloch function.

In cellular method the crystals are considered as divided into unit cells while the atom resides in the center, and such a cell is known as Wigner-Seitz cell. To ensure that the function ψ_k satisfies the Bloch form $\psi_k = e^{i\mathbf{k}\cdot\mathbf{r}} u_k$ it is necessary that u_k be periodic, i.e. u_k be the same on opposite faces of the cell.

Despite its usefulness, the cellular method is greatly oversimplified, and is not currently much in use.

Chapter 5

Density Functional Theory (DFT)

Chapter 5

Density Functional Theory (DFT)

5.1 Basic Idea of DFT

Density functional Theory is quite successful theory which mostly used for calculating and determining the structure of atoms, molecules and solids. One can have the quantitative understanding of material properties from this theory while using fundamental laws of quantum mechanics.

Traditional electronic structure methods used to find approximate solutions to the Schrodinger Equation of N interacting electrons moving in an external electrostatic potential. The computational complexity of the many-body Schrödinger equation means that a solution is beyond current or foreseeable technologies for almost all material problems. However, DFT allows us to sidestep that computational difficulty by focusing on the electron density. The underlying principle of DFT is that the total energy of the system is a unique functional of the electron density [6], hence it is unnecessary to compute the full many-body wave function of the system.

The exact functional dependence of the energy on the density is still unknown. Kohn & Sham [7] transformed this DFT problem of computing the ground state energy and particle density of an N -electron system to that of solving a set of independent-particle equations.

These Kohn–Sham equations consist of N single-particle (three-dimensional) Schrödinger-like equations with a modified effective potential which are easier to solve than the original ($3N$ -dimensional) many-body problem. The modified potential is itself a functional of the total particle density and contains correlation of the particles. No expression for this exchange–correlation (XC) potential is known.

The first general approximation for exchange and correlation was the local density approximation (LSDA) [7, 13].

The main equation of DFT are the Kohn-Sham equations where KS operator is one electron operator:

$$h_{i}^{KS} = -\frac{1}{2} \nabla_i^2 - \sum_k^{nuclei} \frac{Z_k}{|r_i - r_k|} + \int \frac{\rho(r')}{|r_i - r'|} dr' + V_{sc} \quad (6.1)$$

Where the exchange – correlation potential is defined as

$$V_{xc} = \frac{\partial E_{xc}}{\partial \rho}$$

Where V_{xc} is functional derivative. One-electron operator for which the expectation value of the KS Slater determinant is E_{xc}

5.2 Parameters Used

DFT is a method to solve for the electronic structure and energetics of arbitrary materials. It is exact for the ground state but in practice, accuracy depends on choice of parameters, the type of material, the property to be studied and whether the simulated crystal is a good approximation of reality.

Computational Parameters used in Density function theory are

- Kinetic Energy (E_k) cutoff
- Charge density cutoff
- Ionic minimization threshold

Chapter 6

Calculation of Band Energy

Chapter 6

Calculation of Band Energy

6.1 Calculation for K-P Model

6.1.1 Generation of y versus αa Data

Following Codes have been written in Python to generate about 2000 data points for the function $y(= \frac{P}{\alpha a} \sin \alpha a + \cos \alpha a)$ against αa with potential barrier strength of $P = 1.5\pi$.

```
from _csv import writer

import numpy as np
import math
import matplotlib.pyplot as plt
import csv

#Code for generating data points to plot output function y vs alpha_a corresponding to p=3pi/2

p=3*np.pi/2
x=[]          #values for alpha_a
y=[]          #values for function y

i=math.radians(-820)
while i<= math.radians(820):
    if i!=math.radians(0):
        x.append(i)
        y.append(np.sin(i)*(p/(i))+np.cos(i))
    else:
        x.append(i)
        y.append(np.sin(i)*(p/(i)) + np.cos(i))
    i=i+math.radians(0.8)

# plotting data for corresponding x and y

plt.plot(x,y)
plt.show()

#Creating .csv file

with open('mycsv.csv', 'w' , newline='') as f:
    fieldnames =['x_axis' , 'y_axis']
    thewriter = csv.DictWriter(f, fieldnames=fieldnames)

    thewriter.writeheader()
    for i in range(len(x)):
        thewriter.writerow({'x_axis' : x[i], 'y_axis' : y[i]})
```

y vs αa data are also generated for $P= 0.25\pi, 0.5\pi, 0.75\pi, \pi, 1.25\pi, 1.75\pi, 2\pi, 2.25\pi, 2.5\pi, 2.75\pi, 3\pi, 3.25\pi, 3.5\pi, 3.75\pi$ & 4π .

We cannot show this data here due to space limitation.

6.1.2 Plotting y versus αa Data

The generated $y \left(= \frac{P}{\alpha a} \sin \alpha a + \cos \alpha a \right)$ vs αa data for $P = 1.5\pi$ have been plotted using Igor Pro 8 software as shown in Fig. 6.1.

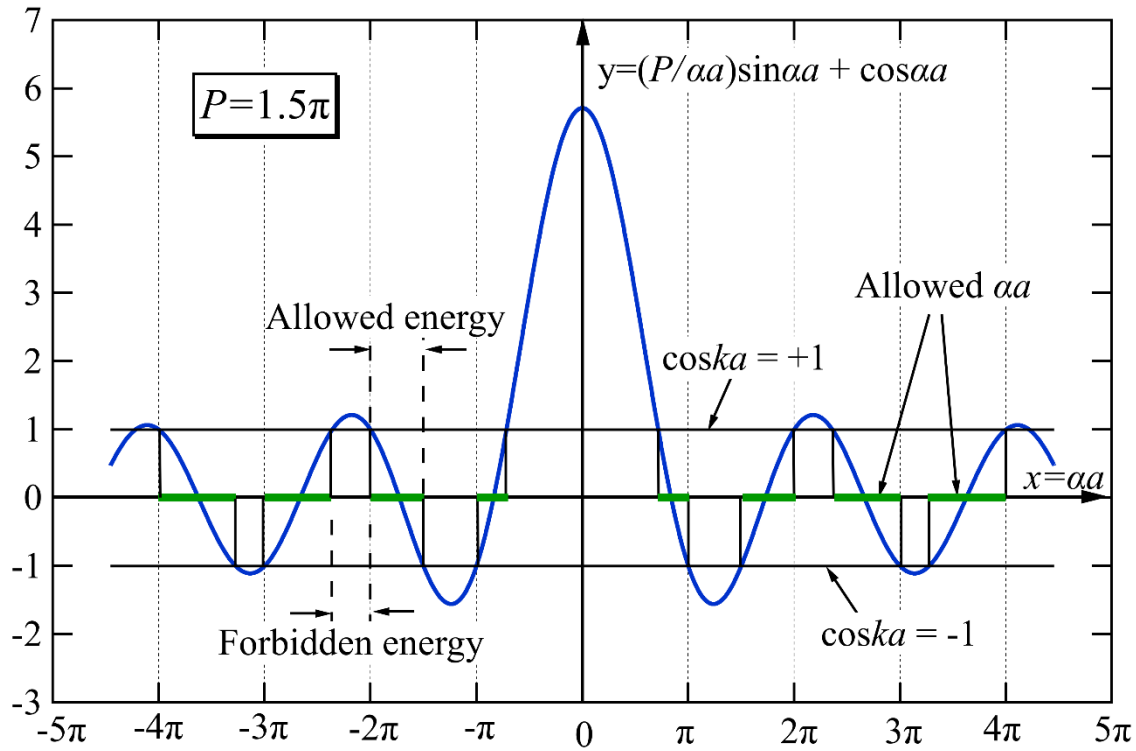


Figure 6.1: $\left(\frac{P}{\alpha a} \sin \alpha a + \cos \alpha a \right)$ versus αa curve for $P = 1.5\pi$.

6.1.3 Band Energy Calculation

The equation $E = \frac{\alpha^2 \hbar^2}{2m} = \frac{(\alpha a)^2 \hbar^2}{2ma^2}$ is used to calculate the band energy E .

The allowed energy E as a function of the wave number k is then calculated. The values of k are calculated using the allowed values of $\cos ka$, which are nothing but the allowed y values (within the range ± 1) of the previous graph.

We write the following formulas in the Igor pro 8 Procedure window to calculate $E - ka$ data for the first energy band.

$a1=4e-10$

$\text{apha_1}=(\alpha_1_a1/a1)$

$h_cut_1=1.05459e-34$

$mass_1=9.10956e-31$

$E_1=(\text{apha_1}^2)*(h_cut_1^2)/2/mass_1/(1.60219e-19)$

$ka_1=\text{acos}(\cos_ka_1)/\pi$

$\text{minus_ka_1}=-ka_1$

$\text{minus_E_1}=E_1$

The calculated $E - ka$ data for the first energy band are shown in Table 6.1.

Table 6.1: Various data including $E - ka$ data for the 1st energy band.

point	α_1_a1	$a1$	apha_1	h_cut_1	$mass_1$	E_1	\cos_ka_1	ka_1	minus_E_1	minus_ka_1
0	2.248124062	4.00E-10	5620310155	1.05E-34	9.11E-31	1.203500985	1	0	1.203500985	0
1	2.262131066	4.00E-10	5655327665	1.05E-34	9.11E-31	1.218544601	0.967294251	0.081633421	1.218544601	-0.081633421
2	2.276138069	4.00E-10	5690345173	1.05E-34	9.11E-31	1.233681656	0.928045311	0.121488132	1.233681656	-0.121488132
3	2.290145073	4.00E-10	5725362683	1.05E-34	9.11E-31	1.24891215	0.888965066	0.151425087	1.24891215	-0.151425087
4	2.304152076	4.00E-10	5760380190	1.05E-34	9.11E-31	1.264236082	0.850058513	0.176566477	1.264236082	-0.176566477
5	2.31815908	4.00E-10	5795397700	1.05E-34	9.11E-31	1.279653453	0.81133061	0.198743666	1.279653453	-0.198743666
6	2.332166083	4.00E-10	5830415208	1.05E-34	9.11E-31	1.295164262	0.77278628	0.218862456	1.295164262	-0.218862456
7	2.346173087	4.00E-10	5865432718	1.05E-34	9.11E-31	1.31076851	0.734430405	0.2374494	1.31076851	-0.2374494
8	2.36018009	4.00E-10	5900450225	1.05E-34	9.11E-31	1.326466196	0.69626783	0.254842594	1.326466196	-0.254842594
9	2.374187094	4.00E-10	5935467735	1.05E-34	9.11E-31	1.342257322	0.658303357	0.271274416	1.342257322	-0.271274416
10	2.388194097	4.00E-10	5970485243	1.05E-34	9.11E-31	1.358141885	0.62054175	0.28691274	1.358141885	-0.28691274
11	2.402201101	4.00E-10	6005502753	1.05E-34	9.11E-31	1.374119888	0.58298773	0.30188356	1.374119888	-0.30188356
12	2.416208104	4.00E-10	6040520260	1.05E-34	9.11E-31	1.390191329	0.545645976	0.316284342	1.390191329	-0.316284342
13	2.430215108	4.00E-10	6075537770	1.05E-34	9.11E-31	1.406356209	0.508521125	0.330192374	1.406356209	-0.330192374
14	2.444222111	4.00E-10	6110555278	1.05E-34	9.11E-31	1.422614526	0.471617768	0.343670218	1.422614526	-0.343670218
15	2.458229115	4.00E-10	6145572788	1.05E-34	9.11E-31	1.438966284	0.434940453	0.356769417	1.438966284	-0.356769417
16	2.472236118	4.00E-10	6180590295	1.05E-34	9.11E-31	1.455411479	0.398493683	0.369533083	1.455411479	-0.369533083
17	2.486243122	4.00E-10	6215607805	1.05E-34	9.11E-31	1.471950113	0.362281916	0.381997763	1.471950113	-0.381997763
18	2.500250125	4.00E-10	6250625313	1.05E-34	9.11E-31	1.488582186	0.326309561	0.394194815	1.488582186	-0.394194815
19	2.514257129	4.00E-10	6285642823	1.05E-34	9.11E-31	1.505307697	0.290580981	0.406151435	1.505307697	-0.406151435
20	2.528264132	4.00E-10	6320660330	1.05E-34	9.11E-31	1.522126647	0.255100494	0.417891445	1.522126647	-0.417891445
21	2.542271136	4.00E-10	6355677840	1.05E-34	9.11E-31	1.539039036	0.219872364	0.429435909	1.539039036	-0.429435909

22	2.556278139	4.00E-10	6390695347	1.05E-34	9.11E-31	1.556044862	0.18490081	0.440803614	1.556044862	-0.440803614
23	2.570285143	4.00E-10	6425712858	1.05E-34	9.11E-31	1.573144129	0.150190001	0.452011458	1.573144129	-0.452011458
24	2.584292146	4.00E-10	6460730365	1.05E-34	9.11E-31	1.590336833	0.115744053	0.463074763	1.590336833	-0.463074763
25	2.59829915	4.00E-10	6495747875	1.05E-34	9.11E-31	1.607622976	0.081567034	0.47400753	1.607622976	-0.47400753
26	2.612306153	4.00E-10	6530765383	1.05E-34	9.11E-31	1.625002557	0.047662957	0.484822659	1.625002557	-0.484822659
27	2.626313157	4.00E-10	6565782892	1.05E-34	9.11E-31	1.642475578	0.014035787	0.495532124	1.642475578	-0.495532124
28	2.64032016	4.00E-10	6600800400	1.05E-34	9.11E-31	1.660042036	-0.019310568	0.506147127	1.660042036	-0.506147127
29	2.654327164	4.00E-10	6635817910	1.05E-34	9.11E-31	1.677701934	-0.05237225	0.516678235	1.677701934	-0.516678235
30	2.668334167	4.00E-10	6670835417	1.05E-34	9.11E-31	1.695455269	-0.085145457	0.527135496	1.695455269	-0.527135496
31	2.682341171	4.00E-10	6705852928	1.05E-34	9.11E-31	1.713302045	-0.117626442	0.537528542	1.713302045	-0.537528542
32	2.696348174	4.00E-10	6740870435	1.05E-34	9.11E-31	1.731242257	-0.149811511	0.547866686	1.731242257	-0.547866686
33	2.710355178	4.00E-10	6775887945	1.05E-34	9.11E-31	1.74927591	-0.181697028	0.558159014	1.74927591	-0.558159014
34	2.724362181	4.00E-10	6810905453	1.05E-34	9.11E-31	1.767403	-0.213279411	0.568414465	1.767403	-0.568414465
35	2.738369185	4.00E-10	6845922962	1.05E-34	9.11E-31	1.785623529	-0.244555135	0.578641917	1.785623529	-0.578641917
36	2.752376188	4.00E-10	6880940470	1.05E-34	9.11E-31	1.803937496	-0.275520735	0.588850272	1.803937496	-0.588850272
37	2.766383192	4.00E-10	6915957980	1.05E-34	9.11E-31	1.822344903	-0.306172799	0.599048535	1.822344903	-0.599048535
38	2.780390195	4.00E-10	6950975487	1.05E-34	9.11E-31	1.840845748	-0.336507978	0.609245908	1.840845748	-0.609245908
39	2.794397199	4.00E-10	6985992998	1.05E-34	9.11E-31	1.859440032	-0.366522979	0.619451886	1.859440032	-0.619451886
40	2.808404202	4.00E-10	7021010505	1.05E-34	9.11E-31	1.878127753	-0.396214567	0.629676361	1.878127753	-0.629676361
41	2.822411206	4.00E-10	7056028015	1.05E-34	9.11E-31	1.896908915	-0.425579569	0.639929743	1.896908915	-0.639929743
42	2.836418209	4.00E-10	7091045523	1.05E-34	9.11E-31	1.915783513	-0.454614872	0.650223095	1.915783513	-0.650223095
43	2.850425213	4.00E-10	7126063032	1.05E-34	9.11E-31	1.934751552	-0.483317422	0.660568295	1.934751552	-0.660568295
44	2.864432216	4.00E-10	7161080540	1.05E-34	9.11E-31	1.953813028	-0.511684226	0.670978225	1.953813028	-0.670978225
45	2.87843922	4.00E-10	7196098050	1.05E-34	9.11E-31	1.972967944	-0.539712354	0.681466998	1.972967944	-0.681466998
46	2.892446223	4.00E-10	7231115557	1.05E-34	9.11E-31	1.992216297	-0.567398936	0.692050245	1.992216297	-0.692050245
47	2.906453227	4.00E-10	7266133068	1.05E-34	9.11E-31	2.01155809	-0.594741165	0.702745459	2.01155809	-0.702745459
48	2.92046023	4.00E-10	7301150575	1.05E-34	9.11E-31	2.03099332	-0.621736295	0.713572439	2.03099332	-0.713572439
49	2.934467234	4.00E-10	7336168085	1.05E-34	9.11E-31	2.05052199	-0.648381646	0.724553865	2.05052199	-0.724553865
50	2.948474237	4.00E-10	7371185593	1.05E-34	9.11E-31	2.070144098	-0.674674598	0.735716033	2.070144098	-0.735716033
51	2.962481241	4.00E-10	7406203102	1.05E-34	9.11E-31	2.089859646	-0.700612596	0.747089852	2.089859646	-0.747089852
52	2.976488244	4.00E-10	7441220610	1.05E-34	9.11E-31	2.10966863	-0.726193149	0.758712191	2.10966863	-0.758712191
53	2.990495248	4.00E-10	7476238120	1.05E-34	9.11E-31	2.129571055	-0.75141383	0.770627761	2.129571055	-0.770627761
54	3.004502251	4.00E-10	7511255627	1.05E-34	9.11E-31	2.149566917	-0.776272276	0.782891802	2.149566917	-0.782891802
55	3.018509255	4.00E-10	7546273138	1.05E-34	9.11E-31	2.169656219	-0.800766189	0.795574058	2.169656219	-0.795574058
56	3.032516258	4.00E-10	7581290645	1.05E-34	9.11E-31	2.189838958	-0.824893337	0.808764882	2.189838958	-0.808764882
57	3.046523262	4.00E-10	7616308155	1.05E-34	9.11E-31	2.210115137	-0.848651553	0.822585035	2.210115137	-0.822585035
58	3.060530265	4.00E-10	7651325663	1.05E-34	9.11E-31	2.230484754	-0.872038736	0.837202361	2.230484754	-0.837202361
59	3.074537269	4.00E-10	7686343172	1.05E-34	9.11E-31	2.25094781	-0.895052849	0.852862327	2.25094781	-0.852862327
60	3.088544272	4.00E-10	7721360680	1.05E-34	9.11E-31	2.271504304	-0.917691923	0.869949754	2.271504304	-0.869949754
61	3.102551276	4.00E-10	7756378190	1.05E-34	9.11E-31	2.292154238	-0.939954055	0.889132455	2.292154238	-0.889132455
62	3.116558279	4.00E-10	7791395698	1.05E-34	9.11E-31	2.312897608	-0.961837408	0.911778391	2.312897608	-0.911778391
63	3.130565283	4.00E-10	7826413208	1.05E-34	9.11E-31	2.333734419	-0.983340214	0.94181586	2.333734419	-0.94181586
64	3.144572286	4.00E-10	7861430715	1.05E-34	9.11E-31	2.354664667	-1	1	2.354664667	-1

The E and k values are then calculated and plotted (Fig. 6.2) for the first band. We have used the similar procedures in order to calculate the band energy for 2nd, 3rd and 4th energy bands.

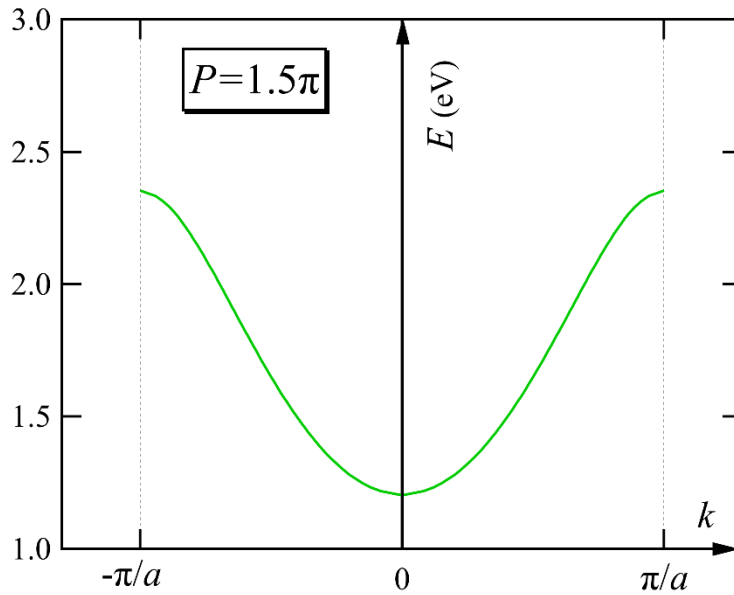


Figure 6.2: $E - k$ curve for the first band with $P = 1.5\pi$, $a = 4 \times 10^{-10}\text{m}$, $m = 9.10956 \times 10^{-31}\text{kg}$.

6.2 DFT-based Calculation for Band Energy of CeAs

We have calculated band energy of cerium arsenide (CeAs) on the basis of first-principles density functional theory (DFT). The calculation was run within the CASTEP code [8] with the generalized gradient approximation (GGA) and the Perdew-Burke-Ernzerhof (PBE) exchange-correlation functional [8, 14].

The face-centered cubic (*fcc*) unit cell of CeAs is shown in Fig. 6.3. It has space group 225 FM-3M with lattice parameter 5.92 \AA at ambient pressure. The calculated the band structure of CeAs along the high symmetry directions in the k -space is shown in Fig. 6.4.

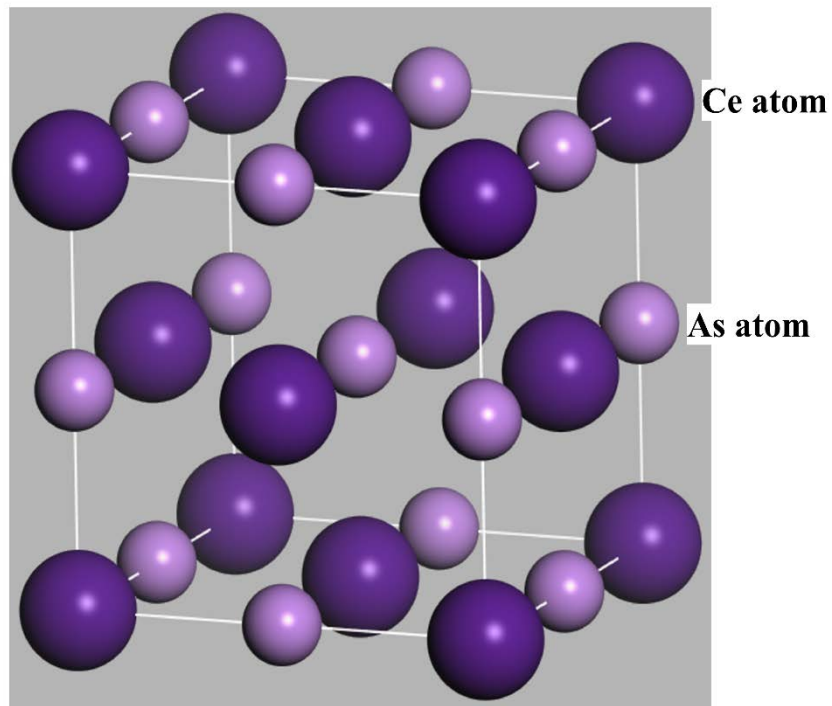


Figure 6.3: Conventional unit cell of CeP.

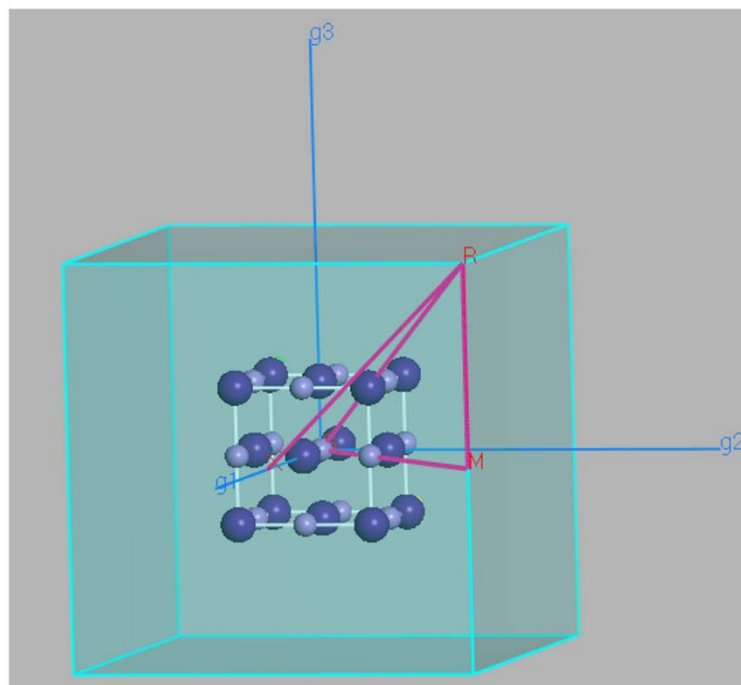


Figure 6.4: High symmetry directions in the reciprocal space of CeAs.

Chapter 7

Results and Discussion

Chapter 7

Results and Discussion

7.1 Band Energy of KP Model

7.1.1 Band Energy versus Wave Number Curves

Fig. 7.1 shows the energy E versus wave number k curves for first four bands with $P = 1.5\pi$, as obtained on the basis of Kronig-Penney model, in the extended zone scheme. The parameter P is defined by $P = \frac{mV_0ab}{\hbar^2}$, where V_0b is the area of the potential barrier. It is observed that the discontinuities in the E versus k curve occur at $k = \pm \frac{n\pi}{a}$ (with $n = 0, 1, 2, 3, \dots$, etc.). Actually, these k values define boundaries of the first, second, third, etc. Brillouin zones.

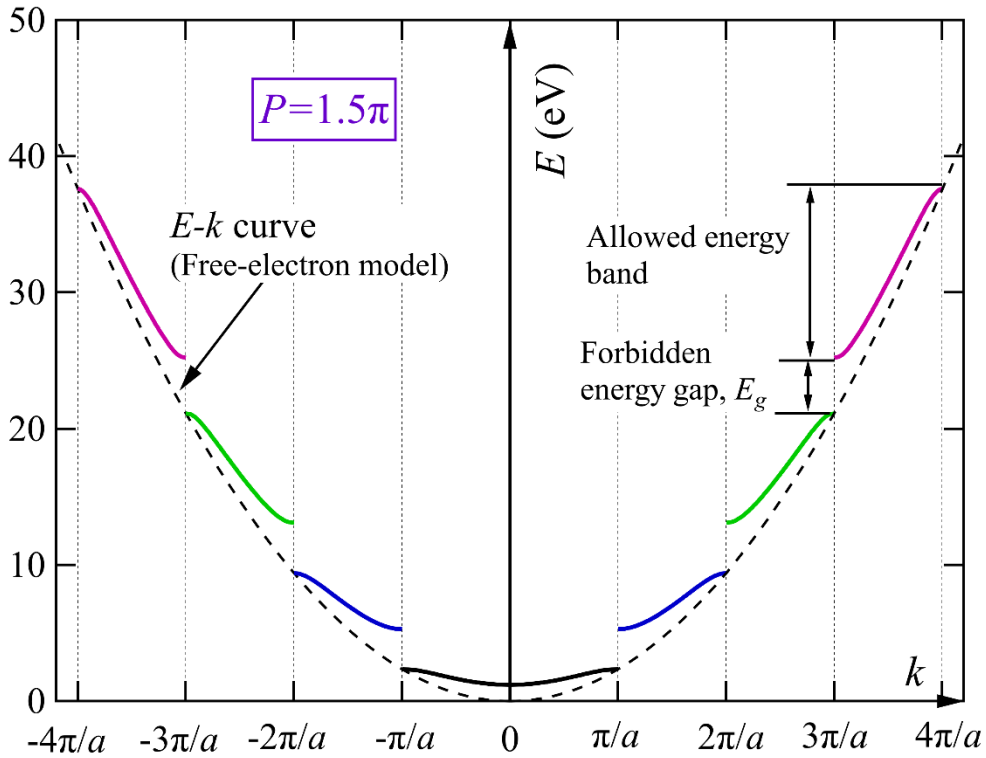


Figure 7.1: $E - k$ curves for first four bands with $P = 1.5\pi$, $a = 4 \times 10^{-10}\text{m}$, $m = 9.10956 \times 10^{-31}\text{kg}$ (solid curves) in the extended zone scheme.

Fig. 7.2 shows that both forbidden energy gap E_g at the zone boundaries and the bandwidth of the allowed energy band increase nonlinearly with the increase of wave number at $P = 1.5\pi$.

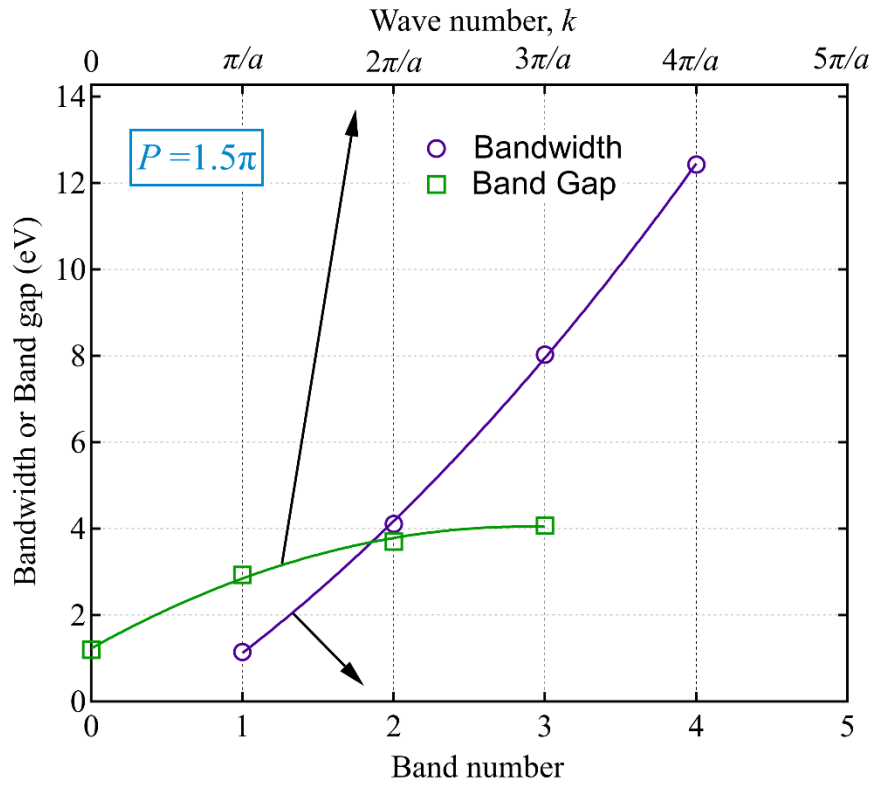


Figure 7.2: Bandwidth as a function of band number (open circles) and band gap as a function of wave number (open squares).

7.1.2 Variation of Band Gap with P

Figure 7.3 shows the calculated band gap as a function of P at various zone boundaries. Non-linear variation of band gap E_g at the zone boundary with the parameter P is found.

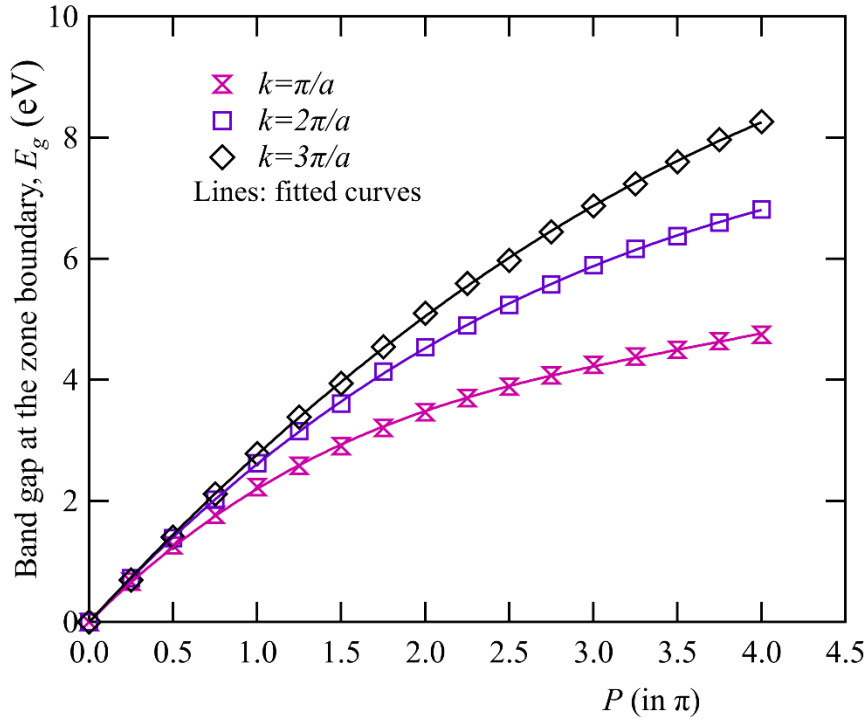


Figure 7.3: Band gap as a function of P at various zone boundaries.

7.2 Band Energy of CeAs based on DFT

We have calculated the band structure of CeAs at ambient pressure (AP) along the high symmetry directions in the Brillouin zones. At first, the geometry (unit cell) at AP has been optimized, and then calculation for the band structure has been started. The calculated energy range was from -36 eV to 18 eV. In order to see the band structure more clearly, the band structure has been plotted between -5 eV to 5 eV (Fig. 7.4). As the valence band and conduction band overlaps along certain direction in the reciprocal space and valence band cross above the Fermi level, thus CeAs is a semi-metal. The occupied valence band of CeAs at ambient pressure lies in the energy range from -4.0 eV to -1.0 eV (Fig. 7.4). The band structure of CeAs at ambient pressure in the wide energy range is shown in Fig. 7.5.

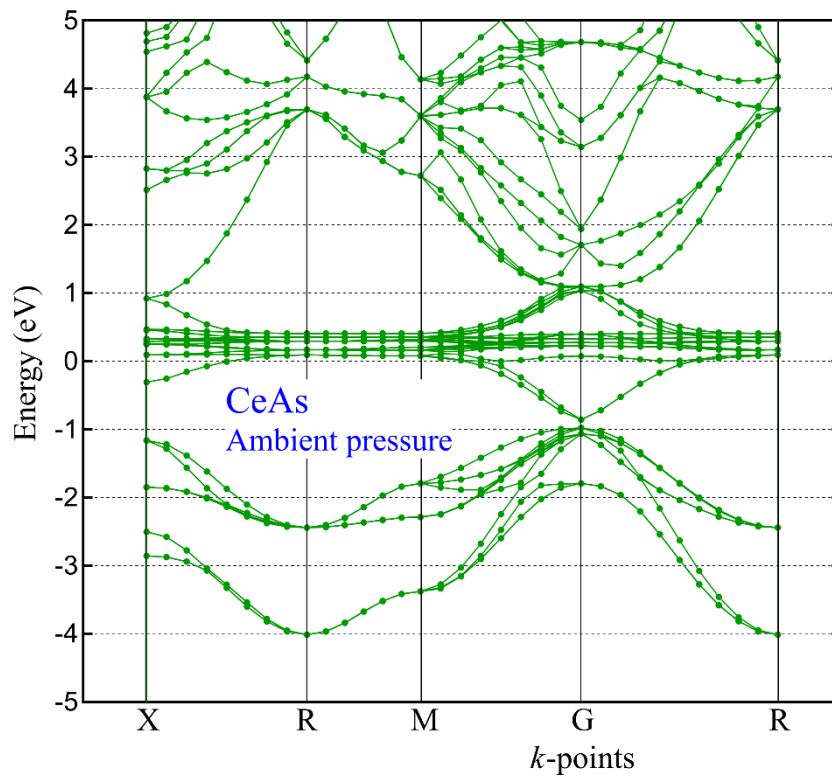


Figure 7.4: Band structure of CeAs at ambient pressure in the narrow energy range.

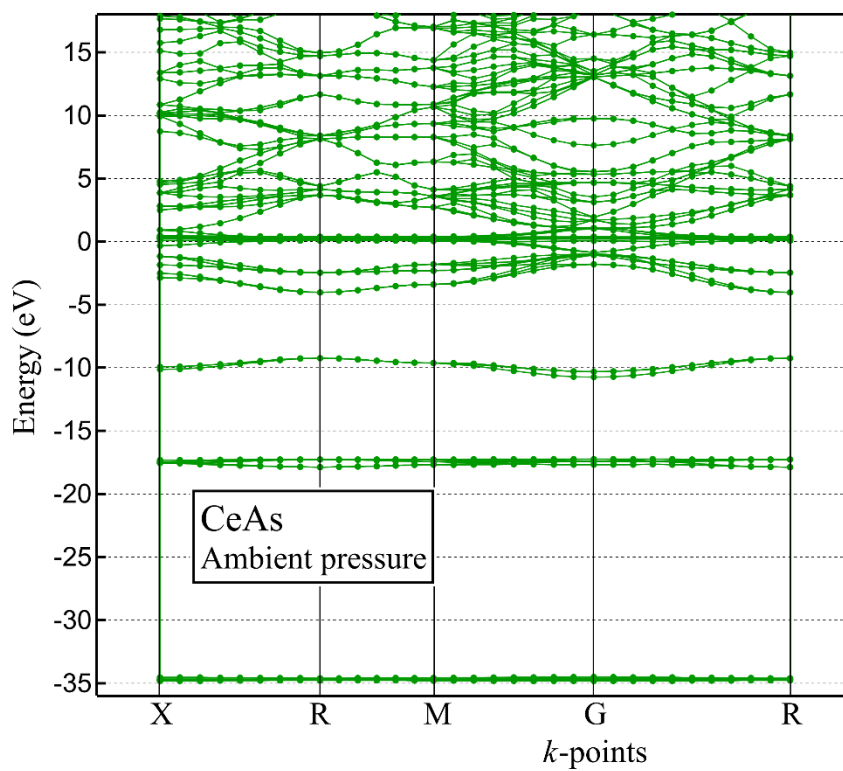


Figure 7.5: Band structure of CeAs at ambient pressure in the wide energy range.

The density of states (DOS) of a material is defined as the number of states per energy range that are available to be occupied by the electrons. It provides the information by which physical properties of the material can be understood. The total density of states (TDOS) and partial density of states (PDOS) of CeAs at normal environmental have also been calculated and the results are shown in Figures 7.6.

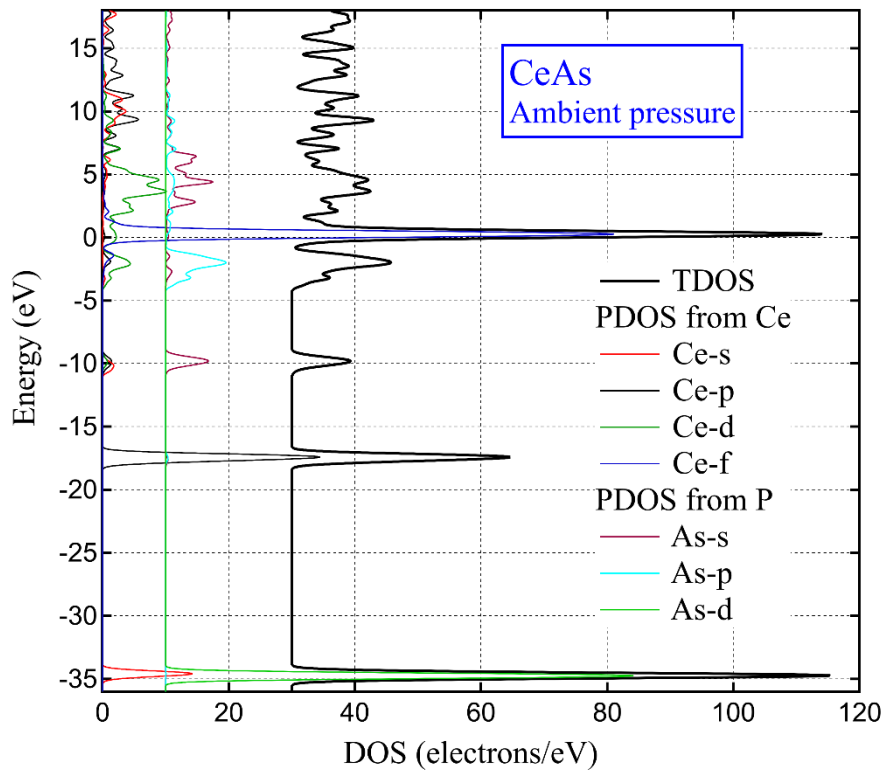


Figure 7.6: Density of states of CeAs at ambient pressure.

Chapter 8

Conclusion

Chapter 8

Conclusion

The main the achievements of this project work are as follows:

- (i) An effort has been made in order to calculate the band structure (in general) adopting the very artificial Kronig-Penney model. The energy E as a function of wave number k for various values of model potential have been calculated.
- (ii) It is found that both the band gap at the zone boundaries and the bandwidth of the allowed energy band increase with the increase of wave number although the increment for the later one is faster the wave number.
- (iii) The band structure, electronic density of states (total and partial) of CeAs at normal pressure have been calculated using CASTEP code on the basis of first-principles density functional theory (DFT). This calculated result shows the semi-metallic character of this compound.
- (iv) The occupied valence band of CeAs lies in the energy range from -4.0 eV to -1.0 eV.

References

1. R. de L. Kronig and W. G. Penney, Proc. Roy. Soc. (London) A 130 (1931) 499.
2. D. A McQuarrie, The Chemical Educator, vol. 1 (1996) S1430-4171.
3. Kittel, C. (2005). *Introduction to solid state physics*, John Wiley & Sons. Inc., New York.
4. *IGOR Pro Version 8.0*, WaveMetrics Inc., PO Box 2088, Lake Oswego, OR 97035, USA.
5. https://www.researchgate.net/publication/341565111_Thomas-Fermi_model
6. P. Hohenberg and W. Kohn, *Inhomogeneous Electron Gas*, Phys. Rev. 136, (1964) B864.
7. W. Kohn and L. J. Sham, *Self-Consistent Equations Including Exchange and Correlation Effects*, Phys. Rev. Vol. 140, No. 4A, (1965) A1133.
8. M D Segall, Philip J D Lindan, M J Probert, C J Pickard, P J Hasnip, S J Clark and M C Payne, *First-principles simulation: ideas, illustrations and the CASTEP code*, J. Phys.: Condens. Matter 14 (2002) 2717–2744.
9. Accelrys, Materials Studio CASTEP manual Accelrys, (Accelrys, 2010), pp. 261-262,
<http://www.tcm.phy.cam.ac.uk/castep/documentation/WebHelp/CASTEP.html>.
10. F. Nilsson and F. Aryasetiawan, *Recent progress in first-principles methods for computing the electronic structure of correlated materials*, Computation, 6(1) (2018) 26.
11. M. Ali Omar: *Elementary Solid State Physics: Principles and Application*, Addison-Wesley Publishing Company, 1975.

12. Neil W. Ashcroft and N. David Mermin: *Solid State Physics*, Saunders College Publishing, 1976.
13. Hasnip, Philip & Refson, Keith & Probert, Matt & Yates, Jonathan & Clark, Stewart & Pickard, Chris. (2014). Density Functional Theory in the Solid State. Philosophical transactions. Series A, Mathematical, physical, and engineering sciences. 372. 20130270. 10.1098/rsta.2013.0270.
14. C. Payne, M. P. Teter, D. C. Allan, T. A. Arias, J. D. Joannopoulos, Iterative minimization techniques for ab initio total energy calculations – molecular-dynamics and conjugate gradients, Rev. Mod. Phys. 64 (1992) 1045–1097.